Article

Climate Chamber Experiment-Based Thermal Analysis and Design Improvement of Traditional Huizhou Masonry Walls

Ling Dong [1,2], Hailong Zhou [3], Hongxian Li [4,*], Fei Liu [3], Hong Zhang [5] and Mohamed Al-Hussein [2]

[1] School of Architecture, Nanjing Tech University, Nanjing 211816, China; dling1@ualberta.ca
[2] Department of Civil and Environmental Engineering, University of Alberta,
  Edmonton, AB T6G 1H9, Canada; malhussein@ualberta.ca
[3] Shandong Tong Yuan Design Group Co., LTD, Jinan 250101, China; hailongzhou@139.com (H.Z.);
  liufei667@139.com (F.L.)
[4] School of Architecture and Built Environment, Deakin University, Geelong 3220, Australia
[5] School of Architecture, Southeast University, Nanjing 210096, China; zhang555@aliyun.com
* Correspondence: hong.li@deakin.edu.au

Abstract: Supported by thousands of years of history, traditional Huizhou buildings have played a vital role, both functionally and culturally, as residential buildings in China. Masonry walls are one of the key building components of a Huizhou building; however, the traditional Huizhou masonry wall structure, predominantly a hollow brick structure, cannot meet the local building energy code requirements, and thus needs to be improved. Within this context, the present research measures the actual thermal performance of traditional Huizhou masonry walls for historical buildings and new-built buildings, which results in mean thermal transmittances of 1.892 $W/m^2 \cdot K$ and 2.821 $W/m^2 \cdot K$, respectively, while the local building energy code requires a minimum thermal transmittance of 1.500 $W/m^2 \cdot K$. In order to improve the thermal performance of traditional Huizhou masonry walls, four design scenarios for wall insulation are proposed and tested in a climate chamber: (1) hollow brick wall with inorganic interior insulation mortar, (2) solid brick wall with inorganic interior insulation mortar, (3) hollow brick wall with foamed concrete, and (4) hollow brick wall with foamed concrete plus inorganic interior insulation mortar. The experiment results indicate that, among the four proposed design scenarios, only scenario 4 can significantly improve the thermal performance of Huizhou masonry walls and meet the building energy code requirements, with a mean thermal transmittance of 1.175 $W/m^2 \cdot K$. This research lays the foundation for improving the thermal performance of Huizhou masonry walls with new insulation and construction technology, thereby helping to improve the quality of life of Huizhou residents while respecting the cultural significance of the traditional Huizhou building.

Keywords: thermal analysis; Huizhou masonry walls; climate chamber experiment

1. Introduction

Huizhou was originally an administrative area in ancient China, located at the junction of the provinces of Anhui, Zhejiang, and Jiangxi, including the cities and counties of Yixian, Shexian, Jixi, Qimen, Xiuning, and Huangshan in the present-day Anhui province, and Wuyuan county in the present-day Jiangxi province. Mountains and river systems are the most notable geographic characteristics of this region, resulting in a humid climate. The average temperature in winter is between 0 °C and 10 °C, while the average temperature in summer is between 25 °C and 30 °C [1],

with Huizhou falling within the hot-summer and cold-winter (HSCW) climate zone in China [2]. Here, buildings must meet the demand for insulation from heat, for shade, and for ventilation in summer, as well as the demand for insulation from the cold in winter. Traditional Huizhou buildings represent one of the most important architectural styles in China due to their specialized artistic and cultural elements. Historic and modern Huizhou buildings are pictured in Figure 1a,b, respectively. The traditional Huizhou building design uses passive design concepts to achieve high thermal performance without any mechanical or electrical devices, and to adapt to the local climate [2]. The courtyard and atrium layout [3,4] and suspended slab construction allow the wind to flow rapidly, thereby lowering the temperature and humidity in summer [5,6]. However, the exterior walls with low thermal insulation performance and poor airtightness result in poor thermal comfort in winter [7].

| (a) | (b) |

Figure 1. (**a**) Historic Huizhou buildings; (**b**) Modern Huizhou buildings.

Exterior walls are the most important building components of traditional Huizhou buildings, not only contributing greatly to the aesthetic appeal, but also offering insulation interfaces for comfortable interior living environments. Traditional Huizhou masonry walls are primarily composed of stone and clay, and this masonry wall construction technology was developed over thousands of years in Huizhou using rich, locally-found material resources. The masonry wall system primarily includes three parts: the foundation, wall body, and cornice. Figure 2a–c represent the typical construction of the masonry exterior walls.

| (a) | (b) | (c) |
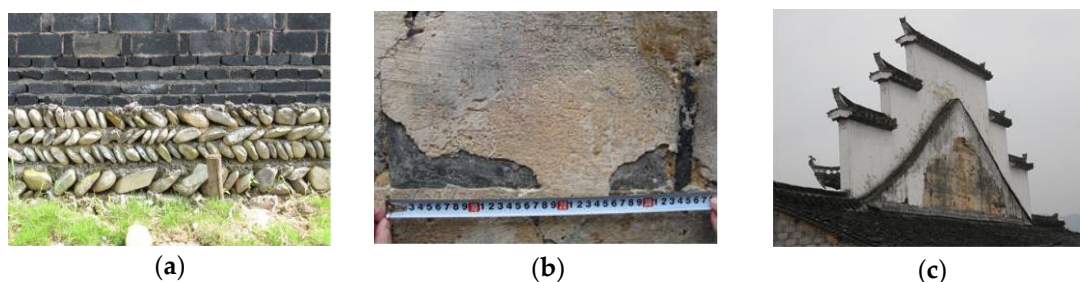
Figure 2. (**a**) Cobblestone foundation; (**b**) Brick wall body; (**c**) Wall cornice construction.

Traditional Huizhou masonry walls are typically composed of bricks, lime, yellow mud, granite, blue stones, and cobblestones [4]. The function of each material is listed in Table 1 for both traditional and modern Huizhou buildings. Table 2 presents the thermal indices of the primary materials used in each [8].

**Table 1.** Typical materials of traditional Huizhou masonry walls.

| Material | Building Type | | Function |
	Historical	Modern	
Brick	✓		Wall body, sheathing brick
Tile	✓	✓	Cornice, wall ridge
Lime	✓	✓	Plaster
Yellow Mud	✓	✓	Filling course, cementing materials
Granite	✓	✓	Lintels, wall foundation
Blue Stone	✓	✓	Decoration
Cobblestone	✓	✓	Wall bottom
Cement Brick		✓	Wall body
Cement		✓	Cementing materials

Table 2. Material thermal indices.

Materials		Dry Density (ρ_0) (kg/m^3)	Thermal Conductivity (λ) [W/(m·K)]	Thermal Mass (S) [kJ/(m^2·K)]	Specific Heat Capacity (c) (kJ/kg·K)
Historical building	Clay brick	1700	0.76	9.96	1.05
	Yellow mud	1800	0.93	11.03	1.01
Modern building	Concrete brick	1800	0.81	10.63	1.05
	Concrete mortar	1700	0.93	11.31	1.05

The "hollow" construction method is the most significant characteristic of traditional Huizhou masonry walls. Typical construction techniques for hollow brick walls include: (1) Dou brick construction only, as demonstrated in Figure 3a, and (2) combined Dou–Mian brick construction, as presented in Figure 3b. According to the traditional Chinese brick construction techniques, brick laid vertically is called Dou brick and brick laid horizontally is called Mian brick.

The hollow wall construction (300–500 mm) with air insulation (60–80 mm) improves the thermal performance of the building envelope [5]. However, Li et al. [9] indicated that traditional grey bricks show different isothermal sorption properties to modern bricks, which leads to a corresponding difference in the heat transfer of brick building enclosure structures. Lucchi [10] also points out that standard analytical procedures tend to overestimate the thermal performance of traditional brick masonries. Another challenge for traditional Huizhou masonry wall technology is the imperative to comply with the local building energy code requirements for thermal performance [11].
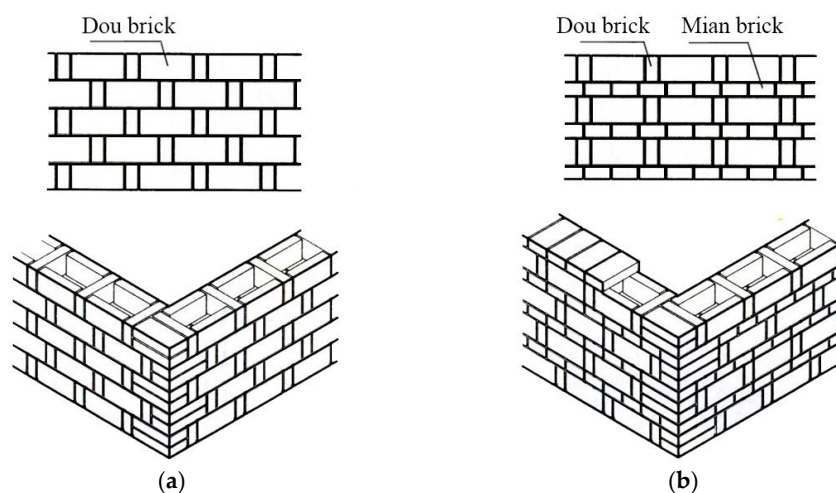
Figure 3. (**a**) Dou brick hollow construction method; (**b**) Dou and Mian combined hollow construction method.

2. Research Objectives and Methodology

The research presented in this paper aims to improve the thermal performance of Huizhou masonry buildings. The detailed research objectives include (1) measuring the actual thermal performance of masonry walls in both traditional and modern Huizhou buildings; (2) proposing insulation scenarios based on the current masonry construction techniques, including inorganic thermal insulation mortar, foamed concrete, and a combination of the two; (3) simulating the thermal performance of the proposed insulation scenarios; (4) conducting climate chamber experiments; and (5) comparing the simulation results with those of the climate chamber experiments for the proposed masonry walls insulation scenarios. The research framework is illustrated in Figure 4, from which it can be observed that site monitoring is used to test the actual thermal performance of traditional Huizhou masonry walls. Based on the monitoring results and analysis, different insulation scenarios are proposed and simulated using THERM software [12]. Climate chamber experimentation is used to verify the results of the proposed design scenarios, while the weather condition parameters of Huizhou are set out as the boundaries of the experimental environment. Chinese national and local building codes constitute the critical design constraints and evaluation criteria for the proposed design scenarios.

The thermal performance of the walls, including thermal resistance and thermal transmittance, is calculated based on the formulas presented in the Chinese Heating Residential Building Energy Saving Code (JGJ/T132-2009) [13], satisfying Equations (1) and (2).

$$R = \frac{\sum_{j=1}^{n} (\theta_{Ij} - \theta_{Ej})}{\sum_{j=1}^{n} q_j} \tag{1}$$

where R is the thermal resistance (or R-value) (m$^2\cdot$K/W); θ_{Ij} is the interior surface temperature of the building envelope at time j ($^\circ$C); θ_{Ej} is the exterior surface temperature of the building envelope at time j ($^\circ$C); and q_j is the heat flux of at time j (W/m^2).

$$K = 1/(R_i + R + R_e) \tag{2}$$

where K is the envelope thermal transmittance (or U-value) (W/m$^2\cdot$K); R_i is the heat transfer resistance of interior surfaces, 0.11 m$^2\cdot$K / W, referring to Chinese code [8]; and R_e is the heat transfer resistance of exterior surfaces, 0.04 m$^2\cdot$K / W, referring to Chinese code [8].
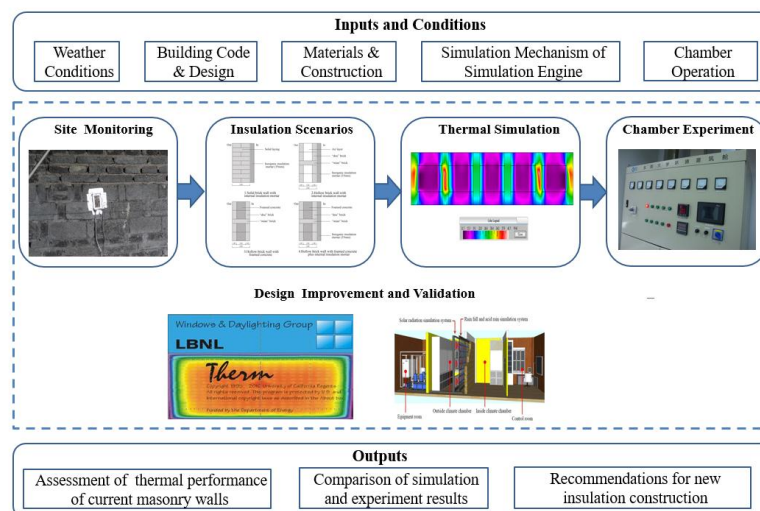

**Figure 4.** Research framework.

2.1. Site Monitoring

The temperature-controlled tank-heat meter method, a convenient approach resulting in accurate data [14,15], was used in the field testing for this research. The temperature-controlled tank-heat meter method provides a stable thermal environment using a hot box and temperature control. The difference between indoor and outdoor temperatures is controlled to be more than 10 °C, ensuring that heat flow is always transmitted from indoors to outdoors. The schematic diagram and instruments of this method are presented in Figures 5 and 6, respectively. As can be seen in Figure 7, six pairs of heat-flow meters were installed on the interior and exterior surfaces of the testing walls correspondingly; each heat-flow meter ws covered with aluminum foil. The actual measurement was conducted during winter, when the outdoor temperature falls between −4.7 °C and 14.5 °C. The hot box temperature was set to 35 °C, and the monitoring data was collected at one-hour intervals. In order to obtain comparable results, the monitoring of traditional and modern building walls was conducted simultaneously by two teams.
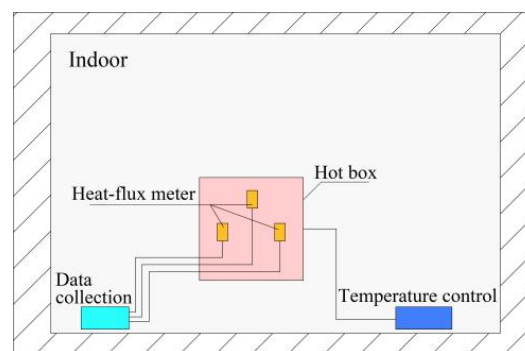
Figure 5. Schematic diagram of the temperature-controlled tank-heat meter method.

Figure 6. Data acquisition instrument.
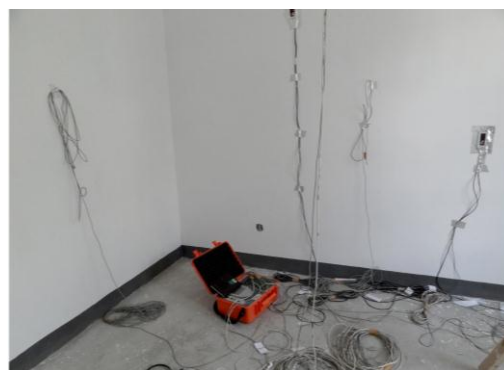
| (**a**) | (**b**) |

Figure 7. (**a**) Monitoring points on the interior surface; (**b**) Monitoring points on the exterior surface.

2.2. Proposed Insulation Scenarios for Huizhou Masonry Walls

In order to improve the thermal performance of buildings constructed with Huizhou masonry design, potential insulation methods are proposed in this paper, based on the current masonry construction techniques, including filling hollow walls using materials with effective heat storage capability and adding an additional insulation layer. According to the research conducted by Wang et al. [16], filling the cavities of hollow blocks with soil or perlite is a feasible way to improve the thermal performance of the walls of solar greenhouses. The results indicate that filling hollow blocks with soil increases the thermal capacity of walls and filling hollow blocks with perlite increases the thermal resistance of walls. These results coincide with the assertion by Song et al. [8] that yellow mud filling improves the thermal performance of Huizhou traditional building masonry walls. Deng et al. [17] presented research on the use of additional insulation layers to improve the thermal performance of traditional building walls; their results indicated that adding expanded polystyrene (EPS) board to the interior or exterior of traditional walls improves the thermal performance.

In the present research, the following considerations are recommended for material selection for filling and additional insulation of Huizhou masonry wall buildings: (1) the insulation materials must be lightweight and easily incorporated into existing wall structures; (2) the insulation materials should meet the required inflammability index; and (3) the insulation materials should be economical and provide constructability. Based on these criteria, two kinds of inorganic insulation materials were chosen for improving the thermal performance of Huizhou masonry brick walls: thermal insulation mortar and foamed concrete.

Inorganic thermal insulation mortar is a widely used and economical insulation material, offering the advantages of a -low inflammability index, constructability, and durability. Inorganic thermal insulation mortar can be used for both interior and exterior insulation construction, and, as such, is suitable for improving the thermal performance of walls in existing buildings. Taking several typical countryside buildings as examples, Zhang [18] conducted research on the thermal performance of exterior walls with different insulation materials; the results indicate that the performance of inorganic thermal insulation mortar is lower than that of organic insulation materials, such as polyurethane (PU) and EPS, but increasing the thickness of inorganic thermal insulation mortar, within the range of 15 mm and 35 mm, can effectively improve thermal performance. The detailed parameters of inorganic thermal insulation mortar, which meets the Chinese code [19] and is used in this research, are displayed in Table 3.

Table 3. Inorganic thermal insulation mortar indices.

| Content		Unit	Technical Index
Dry density		kg/m^3	$\leq$300
Thermal conductivity		W/(m·K)	$\leq$0.065
Compressive strength		MPa	$\geq$0.40
Pressure–shear bond strength		kPa	$\geq$70
Linear Shrinkage		%	$\leq$0.3
Softening coefficient		-	$\geq$0.60
Thermal mass		kJ/(m^2·K)	$\geq$2.30
Frost-resistance	Mass loss rate	%	$\leq$5
	Compressive strength loss rate	%	$\leq$25
Fire resistance level		-	A grade

Foamed concrete is a cement-based, lightweight, porous material, typically made using a pre-foaming method which involves physically foaming and mixing with such materials as cement, aggregate, and admixture. There are two typical foamed concrete products: field-cast foamed cement and prefabricated foamed cement products (blocks or panels). Field-cast foamed cement products are usually used in roof insulation construction, while prefabricated foamed cement products are usually used in wall insulation construction. As a new type of insulation material, foamed concrete

is lightweight and offers fire resistance and frost resistance. According to the relevant literature, the density of foamed concrete [20,21], the utilization efficiency of the foaming agent [22], and the mixing temperature [23] have different impacts on the thermal performance of foamed concrete. The thermal conductivity of foamed concrete, which meets the Chinese foamed concrete code [24], is presented in Table 4.

Table 4. Thermal conductivity of foamed concrete.

Dry Density Grade	A04	A05	A06	A07	A08	A09	A010	A011
Dry Density (ρ_0) (kg/m^3)	300	400	500	600	700	800	900	1000
Thermal Conductivity (λ) (W/m·K)	0.08	0.10	0.12	0.14	0.18	0.21	0.24	0.27

Based on the construction technologies mentioned above, four insulation construction scenarios were proposed for traditional Huizhou masonry walls: (1) solid wall with inorganic insulation mortar, as demonstrated in Figure 8a; (2) hollow wall with inorganic insulation mortar, as presented in Figure 8b; (3) hollow wall with foamed concrete, as displayed in Figure 8c; and (4) hollow wall with foamed concrete plus inorganic insulation mortar, as presented in Figure 8d. The wall samples were designed only with insulation layers, in order to avoid possible disturbance from other layers, such as the protecting coat and the finishing coat. The thickness of the masonry walls (solid and hollow) was 240 mm (the common thickness of new-built Huizhou masonry walls), the thickness of the inorganic interior thermal insulation mortar used the upper limit of the standard code (35 mm) to achieve the best insulation effect, and the thickness of foamed concrete was 120 mm. In this research, an inorganic interior insulation scheme was adopted to reduce the possible damage to present building structure, style, and features. The detailed parameters of materials used in this research are listed in Table 5.

(a)

(b)

(c)

(d)
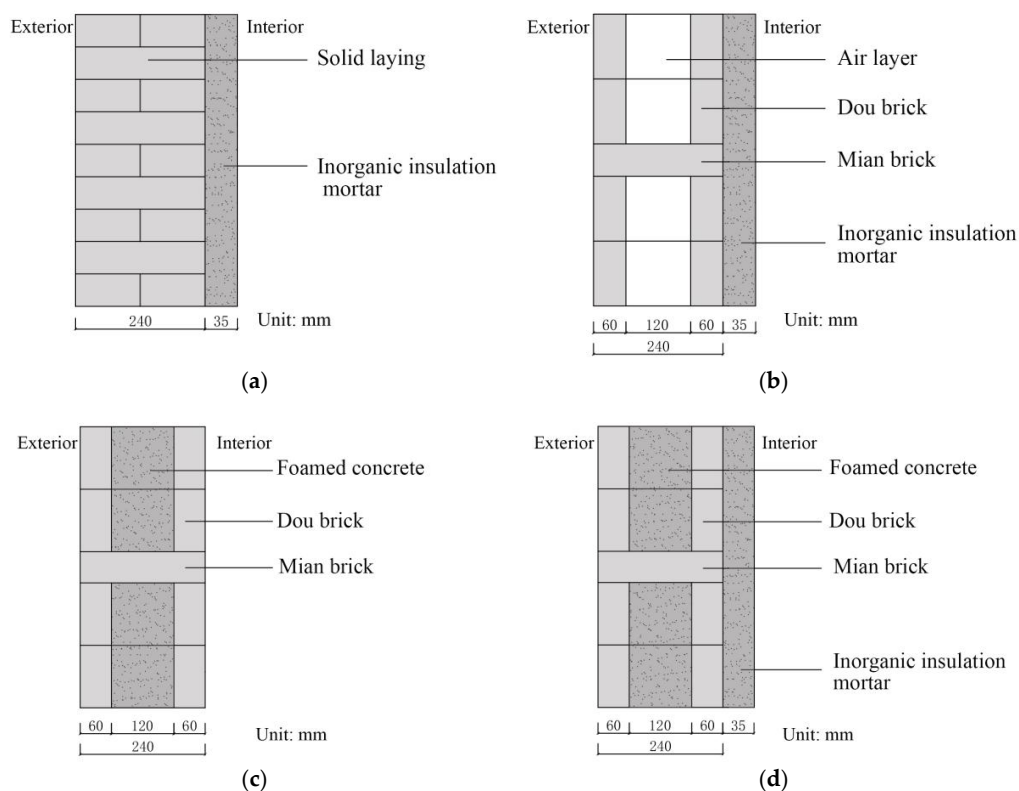
Figure 8. (**a**) Insulation scenario 1: solid wall with inorganic insulation mortar; (**b**) Insulation scenario 2: hollow wall with inorganic insulation mortar; (**c**) Insulation scenario 3: hollow wall with foamed concrete; (**d**) Insulation scenario 4: Hollow wall with foamed concrete plus inorganic insulation mortar.

Table 5. Main materials index.

Material	Dry Density (ρ_0) (kg/m^3)	Thermal Conductivity (λ) [W/(m·K)]	Thermal Mass (S) [kJ/(m^2·K)]	Specific Heat Capacity (c) (kJ/kg·K)
Concrete brick	1800	0.81	10.63	1.05
Foamed concrete	800	0.21	-	-
Inorganic thermal insulation mortar	300	0.065	2.3	-

2.3. Thermal Performance Simulation

There are several software applications available for the performance simulation of buildings, such as HOT2000 and EnergyPlus [25,26]. THERM [12] is a commonly-used software for simulating the thermal performance of building envelopes. It features a finite element method and is based on standards ISO15099 and ISO10077. THERM is also widely used to identify and improve thermal design flaws. In the research presented in this paper, THERM 7.5 was used to simulate the thermal performance of the present Huizhou masonry walls and the proposed insulation construction; the results were compared with the monitoring data. THERM 7.5 was also used to analyze the potential impacts, such as thermal bridge effects. The temperature settings in the simulation corresponded to the actual testing conditions: the interior surface temperature of walls was set to 25 °C, and the exterior surface temperature of walls was set to 5 °C.

2.4. Climate Chamber Experiment

The climate chamber experiment, a reliable method for testing the thermal performance of building components [27,28], was used to test the thermal performance of the proposed insulation scenarios in this research. The overall dimensions of the climate chamber were 6 m × 4 m × 3 m, and the chamber envelope comprised a colored steel plate and polyurethane heat preservation materials. As demonstrated in Figure 9, the climate chamber space was divided into four parts: equipment room, outside climate chamber, inside climate chamber, and control room. Figure 10 depicts a schematic diagram of the climate chamber. Within the climate chamber, the outdoor space, which was controlled by a central computer, was able to mimic different environmental indicators, including temperature, humidity, heat, solar radiation, wind speed, and pressure. The indoor environment was also controlled by a central computer to maintain a suitable temperature, humidity, and wind speed flow. Wall samples were built between the outdoor and indoor spaces, and sensors were installed on the wall samples to collect data over the course of the experiment.
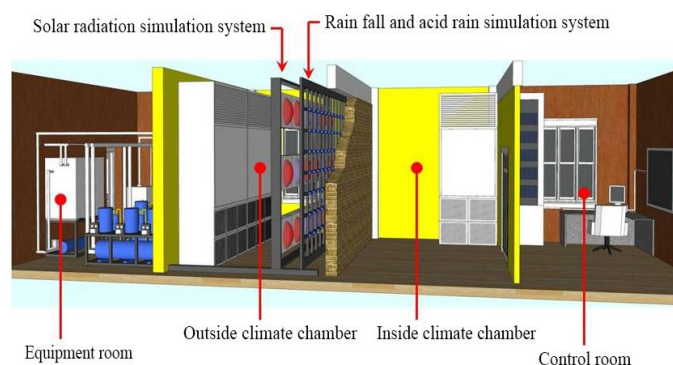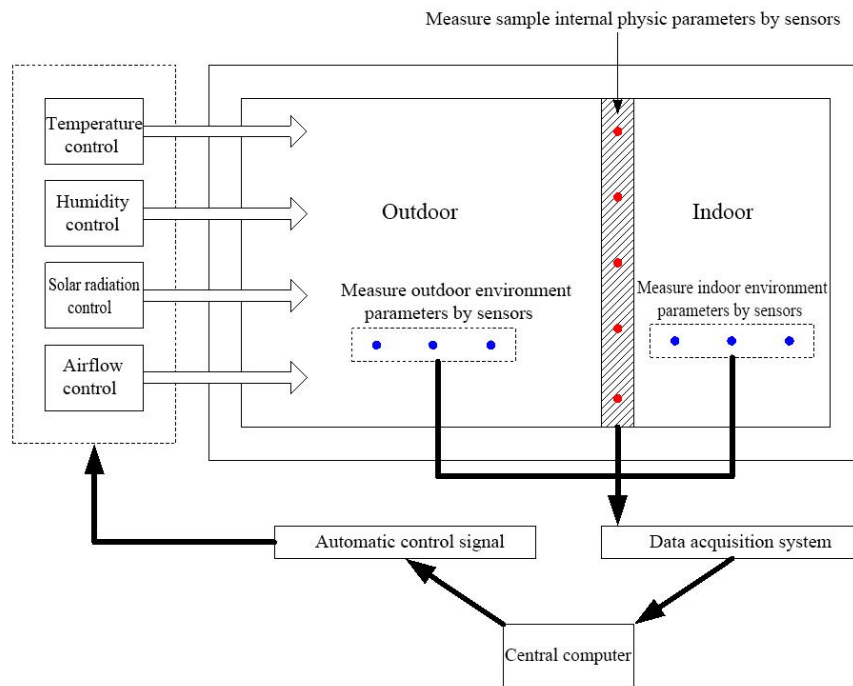

Figure 9. Composition of climate chamber.

Figure 10. Working principles of the climate chamber.

Wall samples with the proposed insulation constructions were built in the climate chamber. The basic composition and dimensions of the wall samples are given in Figure 11. The width of the wall samples was 240 mm, which is the common size of the exterior walls in modern Huizhou buildings. The wall samples were built using solid and hollow construction methods and with the proposed insulation scenarios mentioned before, as demonstrated in Figure 12a–d.
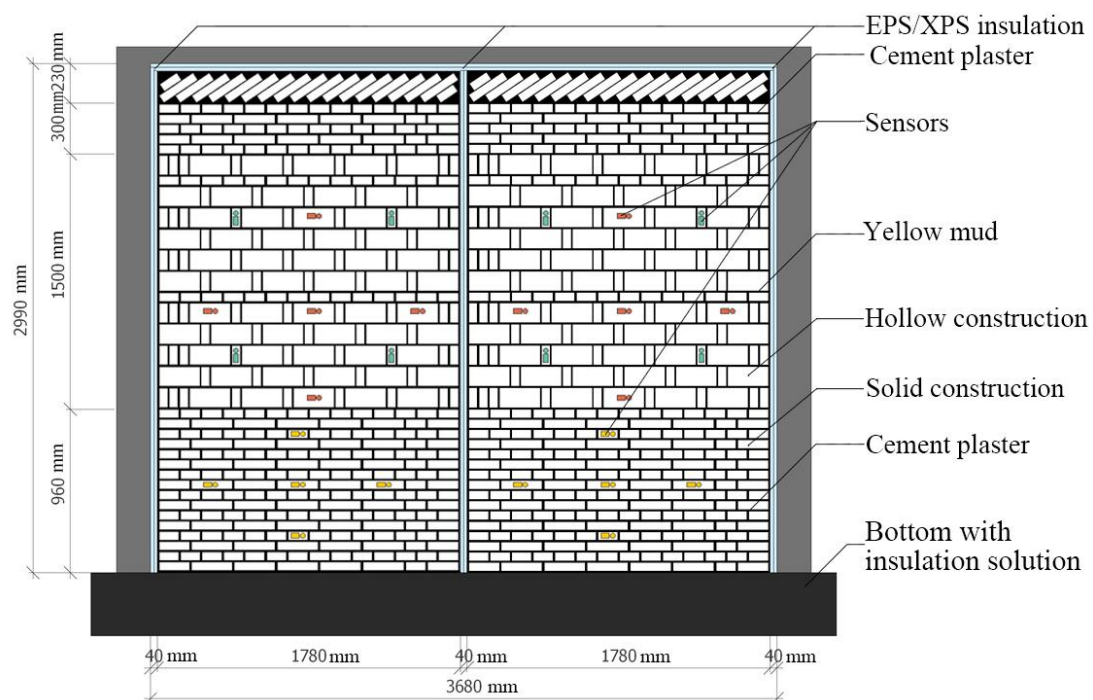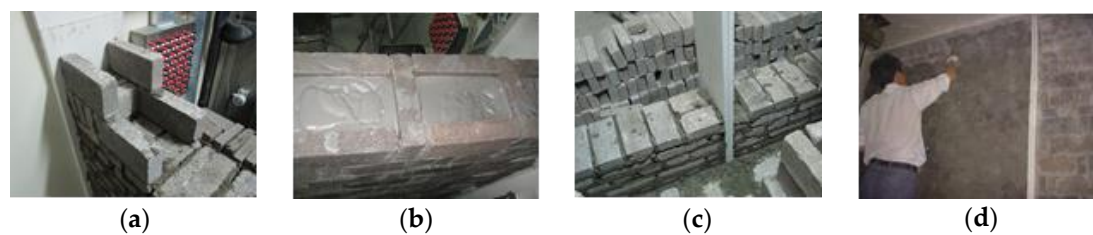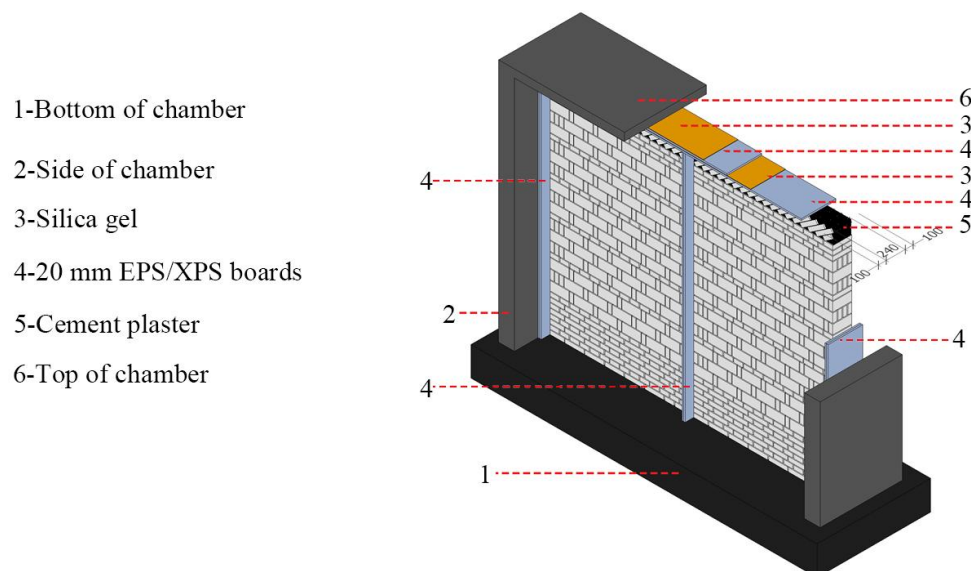

Figure 11. Wall sample construction.

Figure 12. (**a**) Hollow construction; (**b**) Hollow construction with foamed concrete; (**c**) Solid construction; (**d**) Inorganic interior insulation mortar.

The monitoring sensors were installed on both sides of the wall samples to collect the temperature and heat flux data, as demonstrated in Figure 11. In order to prevent the thermal bridge effects between the wall samples and climate chamber, the following solutions were applied in the climate chamber test: (1) EPS or extruded polystyrene (XPS) boards were set up on two sides and the top of walls to prevent heat flux transmission from walls to the climate chamber, and (2) EPS/XPS boards were set up between two wall sample sections to prevent heat exchange, as shown in Figure 13. The duration of the sample walls experiment was 96 h, and the sample data was collected at a time interval of 0.5 h.


1-Bottom of chamber

2-Side of chamber

3-Silica gel

4-20 mm EPS/XPS boards

5-Cement plaster

6-Top of chamber

Figure 13. Specific solutions preventing thermal bridge effects.

3. Results and Analysis

3.1. Monitoring Results and Analysis

Based on the data collected during the site monitoring, the hourly temperature and heat flux changes for both traditional and modern Huizhou walls are presented in Figures 14 and 15. Due to the hot box controlling, the interior surface temperature of the walls remained more stable than the exterior surface temperature of the walls. As indicated in Table 6, the values of heat flux density of traditional and modern buildings were 52.8 W/m^2 and 77.6 W/m^2, respectively, which was obtained by averaging the monitored data. As a result, the traditional building masonry walls with hollow brick construction and yellow mud filling measured a mean thermal transmittance of 1.892 W/m$^2 \cdot$K and a mean thermal resistance of 0.379 m$^2 \cdot$K/W, while the modern building masonry walls with concrete hollow brick construction showed a mean thermal transmittance of 2.821 W/m$^2 \cdot$K and a mean thermal resistance of 0.205 m$^2 \cdot$K/W.

The modern buildings with Huizhou masonry design demonstrated poorer thermal performance than traditional buildings for two reasons: (1) the use of traditional clay brick has been forbidden in China for environmental reasons, and thus fabricated concrete bricks with higher thermal conductivity must be used (0.76 W/m·K for traditional clay brick and 0.81 W/m·K for fabricated concrete brick); and (2) the use of yellow mud has been discontinued as a filling material for hollow brick walls, and no other insulation construction technique is used. The results indicate that the mean thermal transmittance fails to meet the requirements of local building codes in both cases—traditional and modern Huizhou masonry walls [11]—where the minimum requirement under the code is a mean thermal transmittance of 1.500 W/m^2·K.
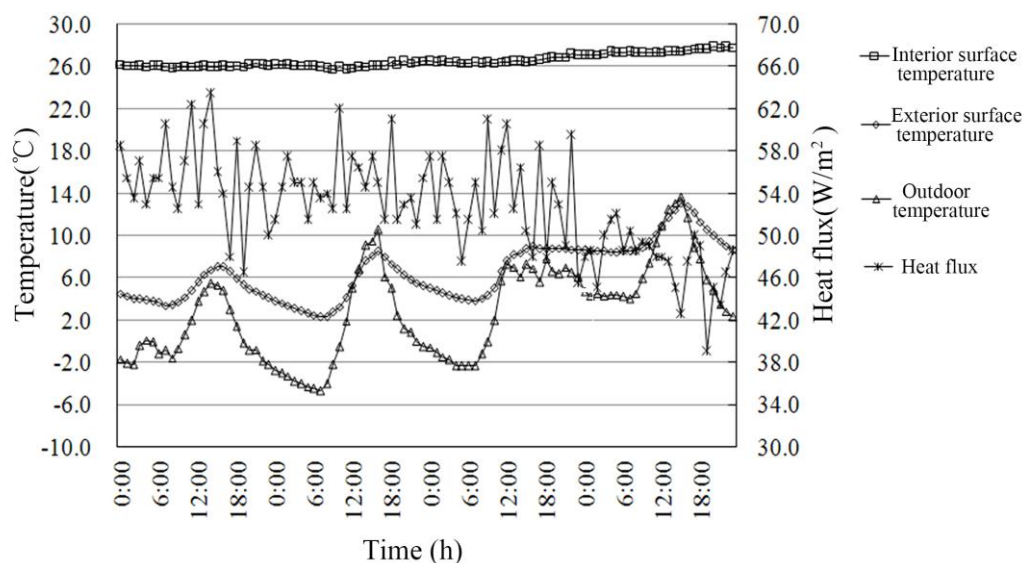
Figure 14. Hourly temperature and heat flux for historical building walls.
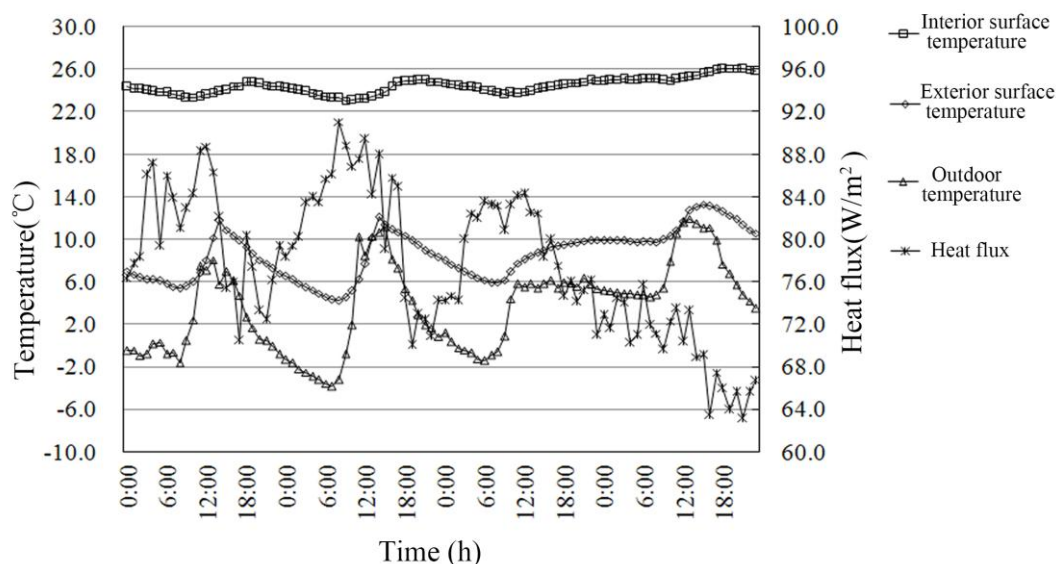
Figure 15. Hourly temperature and heat flux for new-built building walls.

<p style="text-align:center">**Table 6.** Site monitoring results.</p>

	Interior Surface Temperature (θ_I) (°C)	Exterior Surface Temperature (θ_E) (°C)	Heat Flux (*q*) (W/m^2)	Thermal Resistance (*R*) (m^2·K/W)	Thermal Transmittance (*K*) (W/m^2·K)
Historical building	26.6	6.6	52.8	0.379	1.892
New-built building	24.5	8.6	77.6	0.205	2.821

3.2. Simulation Results for the Proposed Insulation Scenarios

Based on the insulation scenarios proposed above, the thermal performance was simulated for each design scenario using THERM 7.5. The thermal parameters for the simulation were set as the values listed in Table 2, and the other simulation environment was set same as the actual monitoring.

As presented in Figures 16–19, the solid wall with inorganic interior insulation mortar resulted in a stable heat flux density with no thermal bridge effect, while in hollow walls, heat flux changed for different insulation scenarios. A thermal bridge is an area or component of an object which has higher thermal conductivity than the surrounding materials. The different colors in the graph indicate the heat flux distribution in the walls, and the part with the higher heat flux density in the graph indicates the thermal bridge. The simulation results of the four proposed scenarios are described as follows: (1) the heat flux value of the solid wall with inorganic interior insulation mortar was the highest among all proposed insulation scenarios, measuring 37.9 W/m^2; (2) the hollow wall with inorganic interior insulation mortar, where the thermal bridge effect is unremarkable, had a low range, flowing between 22 W/m^2 (solid-brick part) and 24 W/m^2 (hollow part); (3) the hollow wall with the foamed concrete insulation, where the thermal bridge effect is clearly seen, had a high heat flux, varying between 16.3 W/m^2 (filling part) and 24.7 W/m^2 (solid-brick part); and (4) the hollow wall with foamed concrete plus inorganic interior insulation mortar, benefiting from double insulation construction, had a much smaller range of heat flux values, which varied between 10.2 W/m^2 (filling part) and 14.3 W/m^2 (solid-brick part). The simulation results for all insulation scenarios are presented in Table 7. According to the results, the hollow wall with foamed concrete plus inorganic interior insulation (Scenario 4) provided the optimal thermal performance, with the highest mean thermal resistance and the lowest mean thermal transmittance (0.757 m^2·K/W and 1.102 W/m^2·K, respectively), while the solid wall with inorganic interior insulation mortar (Scenario 1) provided the lowest thermal performance, with the lowest mean thermal resistance and the highest mean thermal transmittance (0.378 m^2·K/W and 1.895 W/m^2·K, respectively).
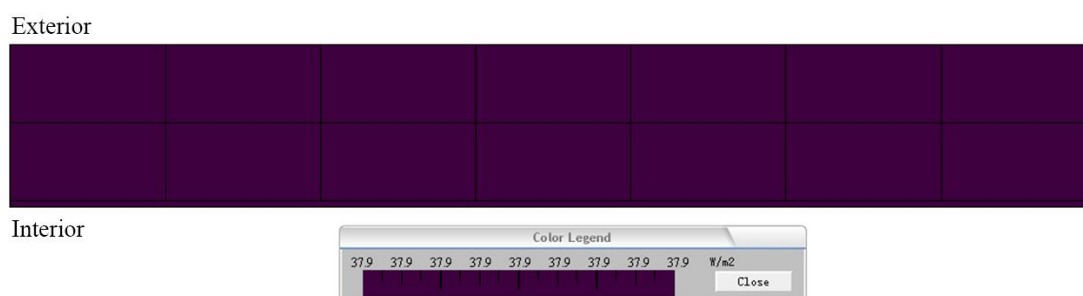

<p style="text-align:center">**Figure 16.** Heat flux distribution graph of scenario 1.</p>
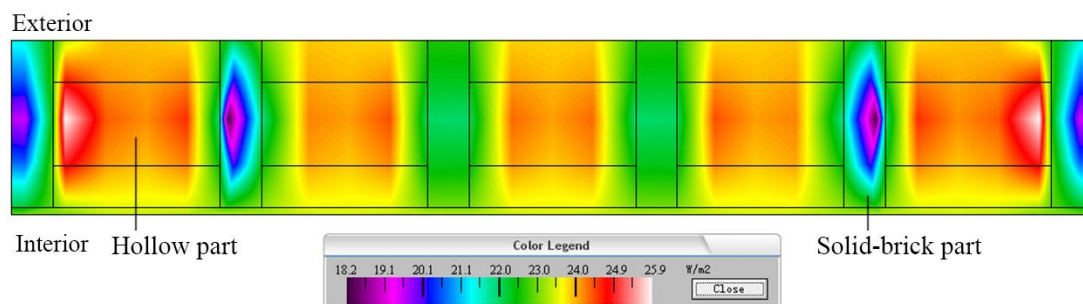
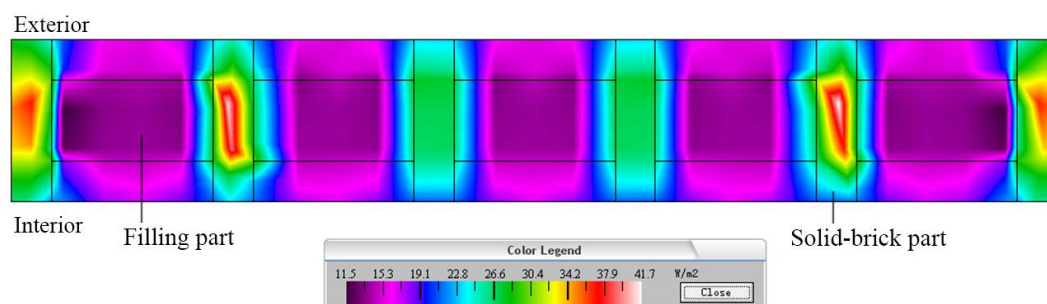**Figure 17.** Heat flux distribution graph of scenario 2.

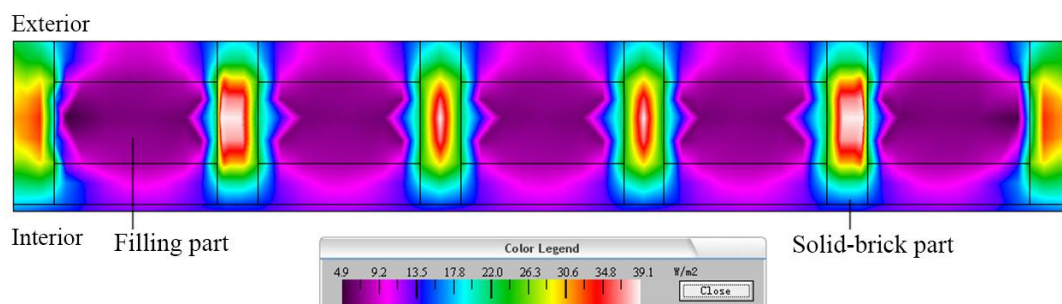**Figure 18.** Heat flux distribution graph of scenario 3.

Figure 19. Heat flux distribution graph of scenario 4.

Table 7. Simulation results.

Insulation Scenarios	Scenario 1	Scenario 2	Scenario 3	Scenario 4
Thermal resistance (*R*) (m^2·K/W)	0.378	0.409	0.416	0.757
Thermal transmittance (*K*) (W/m^2·K)	1.895	1.789	1.767	1.102

3.3. Climate Chamber Experiment Results

Pptimal thermal performance is obtained for with adequate insulation, in accordance with standards, leading to low values in heat flux density, low values in thermal transmittance and high values in thermal resistance. The climate chamber experiment results are presented in Table 8, from which it can be observed that: (1) scenario 1 (solid wall with inorganic interior insulation mortar) offered the lowest thermal performance with the highest mean thermal transmittance and the lowest mean thermal resistance (1.927 m^2·K/W and 0.369 m^2·K/W, respectively) ; (2) scenario 4 (hollow wall with foamed concrete plus inorganic interior thermal insulation mortar) offered the best thermal performance with the lowest mean thermal transmittance and the highest mean thermal resistance (1.175 m^2·K/W and 0.701 m^2·K/W, respectively); and (3) scenario 2 (hollow wall with inorganic

interior insulation mortar) and scenario 3 (hollow wall with foamed concrete) provided similar thermal performance, with mean thermal resistances of 0.403 m^2·K/W and 0.407 m^2·K/W, respectively.

Table 8. Monitoring results of the climate chamber experiment.

Insulation Scenarios	Scenario 1	Scenario 2	Scenario 3	Scenario 4
Interior surface temperature (θ_I) (°C)	21.396	20.802	20.206	23.053
Exterior surface temperature (θ_E) (°C)	9.575	8.226	7.496	8.133
Temperature difference (θ_D) (°C)	11.821	12.576	12.710	14.920
Heat flux (q) (W/m^2)	32.029	30.488	32.844	20.695
Thermal resistance (R) (m^2·K/W)	0.369	0.407	0.403	0.701
Thermal transmittance (K) (W/m^2·K)	1.927	1.795	1.808	1.175

4. Comparison and Conclusions

The climate chamber experiment results were compared with the simulated results, as presented in Figure 20, from which it can be observed that: (1) the simulated and experimental results are similar, and (2) the climate chamber experiment yielded slightly better thermal performance results for the four proposed scenarios than did the simulation. Both the simulation and experiment results indicate that scenario 4 (hollow wall with foamed concrete plus inorganic interior thermal insulation mortar) achieved the best thermal performance, and it can meet the local building energy code requirements. Other scenarios also improve the thermal performance of traditional Huizhou buildings with masonry wall design, but do not meet the local building energy code requirements. In addition, it can be observed that the differences between the simulated and experimented results for scenario 3 and scenario 4 are slightly larger than those between scenario 1 and scenario 2. This is mainly caused by a slumping of the foamed concrete during the construction process (though some measures, as mentioned by the Ministry of Housing and Urban–Rural Development of the People's Republic of China [24], have been carried out), and, as a result, both the thermal conductivity and the density were found to increase.
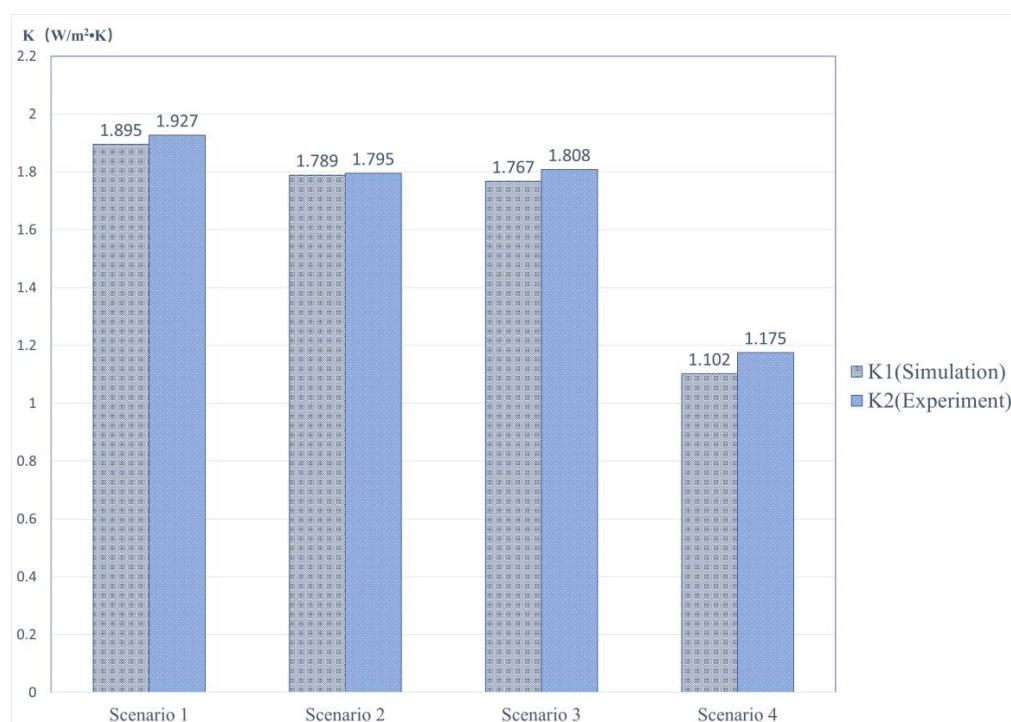
Figure 20. Comparison of simulation and experiment results.

The thermal performance of traditional Huizhou masonry walls with different insulation constructions has been studied. The results from this study suggest that: (1) foamed concrete and inorganic insulation mortar can effectively improve the thermal performance of traditional Huizhou masonry walls; (2) hollow brick walls with foamed concrete plus inorganic interior insulation mortar construction offer the best thermal performance, meeting the local building energy code requirements, and can be considered the optimal choice for local modern Huizhou buildings using masonry wall design; (3) though the walls with a single inorganic interior insulation mortar layer (for both hollow wall and solid wall) fail to satisfy the local building energy code requirements, this material can still be used for improving the thermal performance of existing Huizhou traditional masonry walls. Overall, this study has laid an important foundation for improving the thermal performance of Huizhou masonry walls with new insulation technology, a development which will help to improve the quality of life of Huizhou residents while upholding the cultural significance of traditional Huizhou buildings. In addition, in order to protect historic buildings, further techniques by which to circumvent unnecessary destruction during installation of the inorganic interior insulation mortar layer need to be addressed in future research.

Conflicts of Interest: The authors declare no conflict of interest.

References

1. General Administration of Quality Supervision, Inspection; Quarantine of the People's Republic of China; Ministry of Housing and Urban-Rural Development of the People's Republic of China. *Standard for Climatic Regionalization for Building and Civil Engineering (GB50178-93)*; China Planning Press: Beijing, China, 2005.
2. He, L.L.; Wu, Y.F. Dual Climate Adaptability of Huizhou Ancient Dwellings Based on the ECOTECT. *Build. Energy Effic.* **2013**, *41*, 73–76.
3. Tong, S.S.; Li, H.; Zingre, K.T.; Wan, M.P.; Chang, V.W.-C.; Wong, S.K.; Toh, W.B.T.; Lee, I.Y.L. Thermal performance of concrete-based roofs in tropical climate. *Energy Build.* **2014**, *76*, 392–401. [CrossRef]
4. Jing, H. A Brief Discussion on Passive Energy Saving Technology in Traditional Dwellings in Southern Anhui: Take Dalikeng Village in Wuyuan, Jiangxi Province as an Example. *Zhejiang Constr.* **2014**, *31*, 49–52.
5. Li, J. Investigation of The Passive Energy-saving Technology Alteration of Southern Anhui Traditional Dwellings. *J. Hefei Univ.* **2015**, *25*, 69–72.
6. Song, B.; Bai, L.J.; Liu, Y.; Hu, R.R.; Huang, R.J. Indoor Thermal Environment of Huizhou Traditional Building in Summer. *Build. Energy Effic.* **2015**, *43*, 69–73.
7. Song, B.; Liu, Y.; Liu, D.L.; Hong, Z.G. Field Study on Indoor Thermal Environment in Huizhou Traditional Building in Xidi in Winter. *Archit. Technol.* **2014**, *45*, 1033–1036.
8. General Administration of Quality Supervision Inspection; Quarantine of the People's Republic of China; Ministry of Housing and Urban-Rural Development of the People's Republic of China. *Thermal Design Code for Civil Building (GB50176-1993)*; China Planning Press: Beijing, China, 1993.
9. Li, Y.H.; Xie, H.R.; Wang, J.G.; Li, X.J. Experimental study of the isothermal sorption properties of late Qing and 1980s grey bricks in Wujiang, Suzhou, China. *Front. Archit. Res.* **2013**, *2*, 483–487.
10. Lucchi, E. Thermal transmittance of historical brick masonries: A comparison among standard data, analytical calculation procedures, and in situ heat flow meter measurements. *Energy Build.* **2017**, *134*, 171–184. [CrossRef]
11. Ministry of Housing and Urban-Rural Development of Anhui; General Administration of Quality Supervision, Inspection and Quarantine of Anhui. *Anhui Heating Residential Building Energy Saving Code (DB34/1466-2011)*; Standards Press of China: Beijing, China, 2011.
12. Berkeley Lab: Windows & Daylighting (Building Technology & Urban Systems) 2012. THERM. Available online: https://windows.lbl.gov/tools/therm/software-download (accessed on 16 January 2017).

13.　Ministry of Housing and Urban-Rural Development of the People's Republic of China. *Chinese Heating Residential Building Energy Saving Code (JGJ/T132-2009)*; China Architecture & Building Press: Beijing, China, 2009.

14.　Meng, N.; Li, B.; Chang, W.T.; Hua, Y.W. The Applied Research of Temperature Controlled Tank-Heat Flow Meter Method in Field Testing the Heat Transfer Coefficient of Building Envelope. *J. Jilin Inst. Archit. Civ. Eng.* **2014**, *31*, 29–32.

15.　Kusamaa, Y.; Ishidoya, Y. Thermal effects of a novel phase change material (PCM) plaster under different insulation and heating scenarios. *Energy Build.* **2017**, *141*, 226–237. [CrossRef]

16.　Wang, Y.W.; Li, S.H.; Guo, S.R.; Ma, C.W.; Wang, J.; Sun, J. Analysis of heat transfer properties of hollow block wall filled by different materials in solar greenhouse. *Eng. Agric. Environ. Food* **2017**, *10*, 31–38. [CrossRef]

17.　Deng, Q.Q.; Li, M.S.; Song, B.; Ying, L.D. Energy saving technologies of walls of traditional housing in Beijing rural area. *Build. Energy Effic.* **2014**, *42*, 36–41.

18.　Zhang, X. Effect of Inorganic Heat-insulation Mortar to Building Energy Consumption. *Build. Energy Effic.* **2012**, *40*, 44–49.

19.　General Administration of Quality Supervision, Inspection and Quarantine of the People's Republic of China; Standardization Administration of the People's Republic of China. *Dry-Mixed Thermal Insulating Composition for Buildings (GB/T20473-2006)*; Standards Press of China: Beijing, China, 2006.

20.　She, W.; Chen, Y.Q.; Zhang, Y.S.; Jones, M.R. Characterization and simulation of microstructure and thermal properties of foamed concrete. *Constr. Build. Mater.* **2013**, *47*, 1278–1291.

21.　Pan, Z.H.; Li, H.Z.; Liu, W.Q. Preparation and characterization of super low density foamed concrete from Portland cement and admixtures. *Constr. Build. Mater.* **2014**, *72*, 256–261. [CrossRef]

22.　Cui, Y.Y.; He, H.Z. Influence of Utilization Efficiency of Foaming Agent on Foam Concrete Performance. *J. Build. Mater.* **2015**, *18*, 12–16.

23.　Cui, Y.Y.; He, H.Z. Influence of Temperature on Performances of Foam Concrete. *J. Build. Mater.* **2015**, *18*, 836–846.

24.　Ministry of Housing and Urban-Rural Development of the People's Republic of China. *Foamed Concrete (JG/T 266-2011)*; Standards Press of China: Beijing, China, 2014.

25.　Li, H.X.; Gül, M.; Yu, H.T.; Mohamed, A.-H. Automated energy simulation and analysis for NetZero Energy Home (NZEH) design. *Build. Simul.* **2017**, *10*, 285–296. [CrossRef]

26.　Han, Y.S.; Yu, H.; Sun, C. Simulation-Based Multiobjective Optimization of Timber-Glass Residential Buildings in Severe Cold Regions. *Sustainability* **2017**, *9*, 2353. [CrossRef]

27.　Cho, S.; Kim, S.H. Analysis of the Performance of Vacuum Glazing in Office Buildings in Korea: Simulation and Experimental Studies. *Sustainability* **2017**, *9*, 936. [CrossRef]

28.　Mert Cuce, P. Thermal performance assessment of a novel liquid desiccant-based evaporative cooling system: An experimental investigation. *Energy Build.* **2017**, *138*, 88–95. [CrossRef]